

advances.sciencemag.org/cgi/content/full/7/5/eabd6203/DC1

Supplementary Materials for
Mechanism of C-type inactivation in the hERG potassium channel

Jing Li, Rong Shen, Bharat Reddy, Eduardo Perozo, Benoît Roux*

*Corresponding author. Email: roux@uchicago.edu

Published 29 January 2021, *Sci. Adv.* 7, eabd6203 (2021)
DOI: 10.1126/sciadv.abd6203

The PDF file includes:

Supplementary Text
Figs. S1 to S11

Other Supplementary Material for this manuscript includes the following:

(available at advances.sciencemag.org/cgi/content/full/7/5/eabd6203/DC1)

Movies S1 and S2

Supplementary Text

Spontaneous asymmetric constriction during MD simulations

The conformational state of the selectivity filter is monitored by following the cross-subunit distance between the Ca atoms of G626 from diagonally-opposed subunits (Fig. 1): the distance is ~ 8.1 Å for the conductive conformation. As consistently observed in the first two simulations only with the pore domain (PD), the selectivity filter undergoes a rapid and spontaneous transition toward the constricted conformation (Traj. 1 & 2) (Fig. S1 A). Different from a symmetrical constriction as KcsA channel with two cross-subunit distances both decrease to ~ 5.5 Å (19), the filter constriction of hERG channel is asymmetrical, with one distance drops to about 5 Å (Fig. S1 A and C), and the other one shifts to 7 Å (Fig. S1 A and D). These simulations were extended to 15 and 5 μ s, respectively. The filter stably maintains an asymmetrical constriction despite some transient fluctuations. In the third simulation (Traj. 3) with the PD and four voltage-sensing domains (VSDs), a similar conductive-to-constricted transition toward an asymmetric constricted conformation is also observed (Fig. S1 A).

The K⁺ ion movement coupled with constriction transition

The constriction of the filter is accompanied by change in the number and location of ions in the SF. For a conductive conformation, usually there are three (S0/S2/S4) or two (S2/S4) K⁺ ions bound in the SF of the hERG channel. When the SF switches to a constricted conformation, although the K⁺ ion in S4 site is still stably bound, the K⁺ ions in S0 and S2 sites move toward the extracellular side. As shown in the three μ s-scale unbiased trajectories (Fig. S9), the S4 site is predominantly occupied by a K⁺ ion after the constriction of the filter, whereas the S0 and S1 sites are just occasionally accessed by K⁺ ions.

The coupling of conductive-to-constricted transition and the change of ion occupancy is also confirmed by our 2D-PMF calculations (Fig. S10). In the 2D-PMF, one reaction coordinate z indicates the position of the external K⁺ ion along the z -axis relative to the center of the selectivity filter, and the internal K⁺ ion always occupies the S4 site. The 2D PMFs clearly show that the movement of the external K⁺ ion toward extracellular side is tightly coupled with the conductive-to-constricted transition of the filter, and the displacement of this K⁺ ion from S2 to S1 appears to be the major barrier.

The movement of the ions described above is consistent with the observed increase of the rate of entry into inactivation upon membrane depolarization (Fig. S5). The voltage-dependent increase in the rate can be determined by calculating the state-dependent displacement charge for the two conformations (58). Based on the calculated displacement charge between the conductive and inactivated-constricted states, we find that the relative population of the constricted state increases by about a factor of 14 with a membrane potential of about 100 mV (Fig. S5).

Major structural factors contributing to constriction in the partially open state

There are two potential structural factors increasing the propensity of hERG to be constricted in the partially open state, i.e., the strength of hydrogen bond between Y616 and N629, and the structural arrangement of non-domain-swapped VSDs. The Y616-N629 hydrogen bond is highly conserved among K⁺ channels, although these two residues are more commonly tryptophan and aspartic acid in Kv channels. The strength of the hydrogen bond has a significant impact on the

C-type inactivation rate (29,32,33). On the one hand, a *Shaker*-like mutation N629D in hERG strengthens the hydrogen bond and slows down C-type inactivation substantially. On the other hand, hERG-like mutations in Kv channels weaken the hydrogen bond, such as D447N and W434Y in *Shaker*, and accelerate C-type inactivation (31,33). Another major difference between hERG and most Kv channels is the domain arrangement. In *Shaker*-like Kv channels, the pore domain and voltage-sensing domains are swapped, while in hERG the PD and VSD are not. Accordingly, the S4-S5 linker is much shorter and the PVP kink motif in S5 helix is absent in hERG (Fig. S11). Lastly, the length of S4-S5 linker could affect the range of intracellular gate opening, whereas the PVP kink forms contacts with the residues (V467 and I470 in *Shaker*, equivalent to I100 and F103 in KcsA) that are critical for gates coupling.

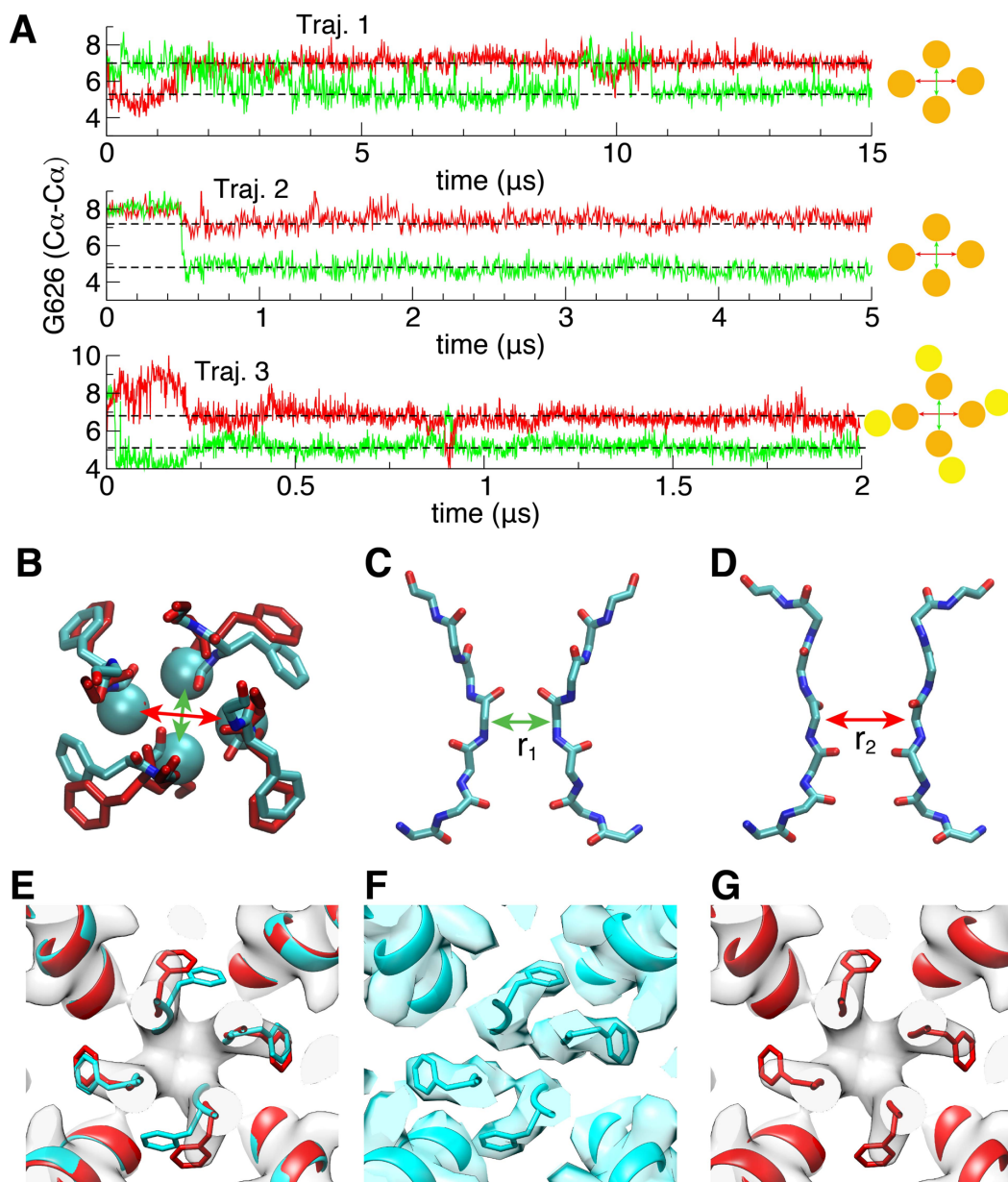


Fig. S1. Spontaneous asymmetric constriction of the selectivity filter in the hERG channel. (A) Time series of the cross-subunit distance between the C α atoms of G626 of diagonally opposed subunits A and C (green), and B and D (red) for three simulations started from the cryo-EM structure (5VA2). Two average distances for the two pairs of subunits are shown in dashed lines. The subunits in the PD and VSDs are illustrated as orange and yellow circles, respectively, on the right. (B-C-D) The C2 model based on an average structure (cyan) from a 300 ns MD trajectory symmetrized by swapping between two opposite subunits is shown from top view overlaid with the cryo-EM structure (red) (B), or from side views (C and D); panels B-C-D are repeated here from **Fig. 1** from the main text for the sake of clarity. (E-F-G) The overlay between the density from C2 model from simulation (cyan) and C4 symmetrical cryo-EM structure (red).

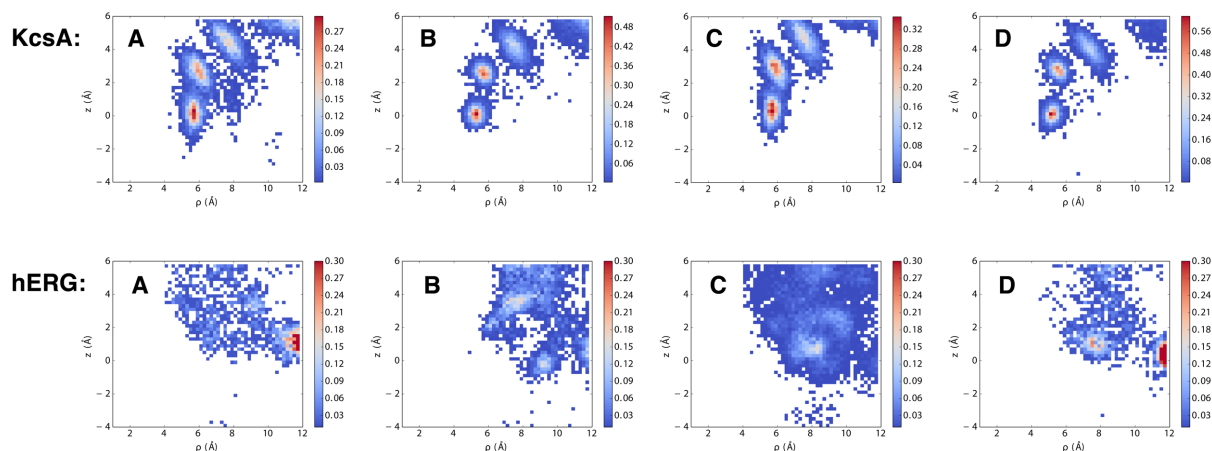


Fig. S2. 2D occupancy map for water molecules behind the selectivity filter in KcsA and hERG. The horizontal reaction coordinate ρ is defined as the distance of the oxygen atom of water molecules with the center of the selectivity filter in the X-Y plane. The vertical reaction coordinate z indicates the position of the oxygen atom of water molecules along the z axis relative to the center of the selectivity filter. The upper panel is the occupancy maps for 4 subunits in KcsA calculated from a trajectory previously reported in a previous study (19). The lower panel is the occupancy maps for 4 subunits in the hERG channel based on the Traj.1 in Fig. S1.

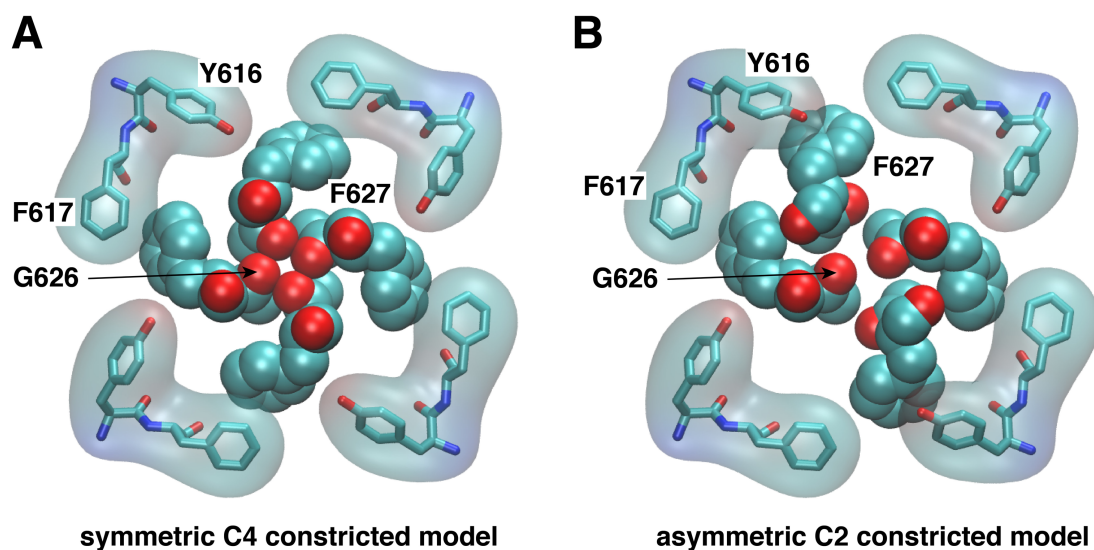


Fig. S3. The structural stability of symmetric and asymmetric constricted conformations. Top views of a hypothetical symmetric constricted (C4) model of hERG generated using the KcsA channel as a template (**A**), and the asymmetric constricted (C2) model based on an average structure (cyan) from a 300 ns MD trajectory of hERG (**B**). Residues G626 and F627 in the selectivity filter are shown in van der Waals sphere representation. Residues Y616 and F617 are illustrated in solid stick and transparent surface representations.

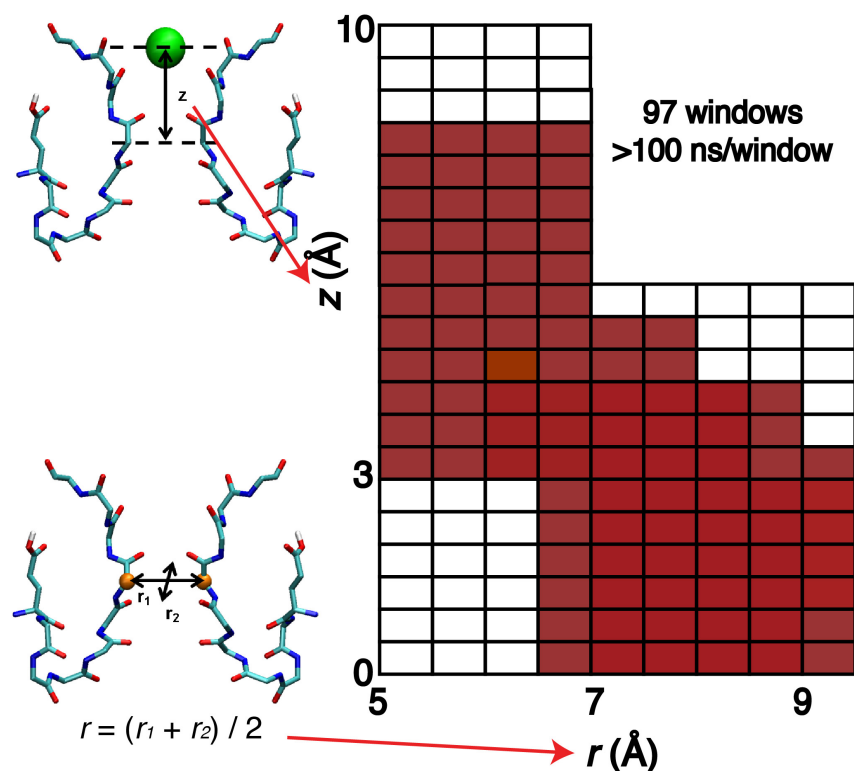


Fig. S4. 2D PMF to calculate free energy difference between conductive and constricted conformations of the selectivity filter. The horizontal reaction coordinate r describes the width of the selectivity filter and is defined as the average cross-subunit distance between the Cα atoms of G626. The vertical reaction coordinate z indicates the position of the external K^+ ion along the z axis relative to the center of the selectivity filter. 97 windows are used to cover such a conformational space, and each window is extended over 100 ns to achieve a converged free energy profile.

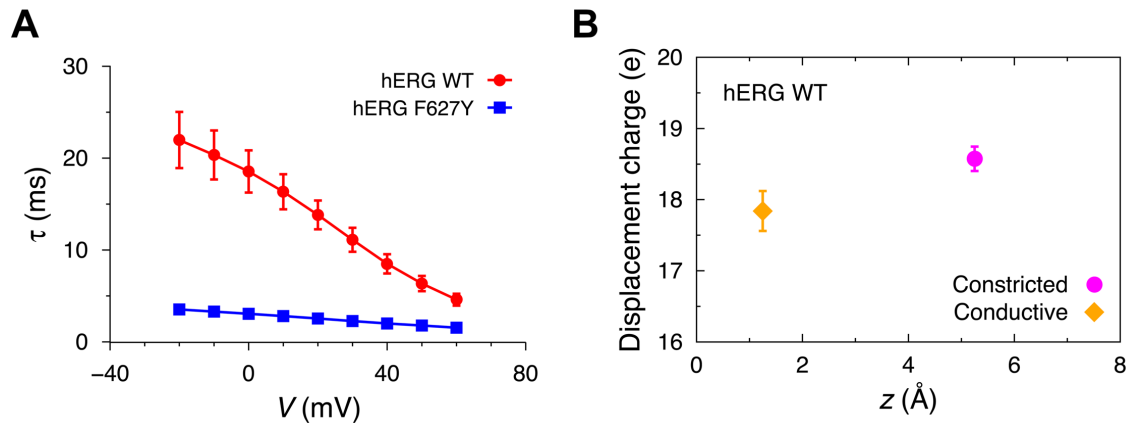


Fig. S5. Voltage dependence of the inactivation kinetics. **(A)** The time constant of inactivation as a function of the voltage for the WT and F627Y channels. Error bars indicate standard deviations (WT: $n = 8$; F627Y: $n = 5$). **(B)** The average displacement charge for the WT channel in the constricted state (magenta circle) and the conductive state (orange diamond). The x-axis shows the restraint center of the z coordinate of the outer K^+ ion in different simulations. Error bars indicate standard deviations ($n = 400$). Using Eq. (1), the change in the average displacement charge $\langle \Delta Q_d \rangle$, going from the conductive and constricted conformations is about 0.7 unit charge. At 100 mV, this corresponds to a population shift of about 14.

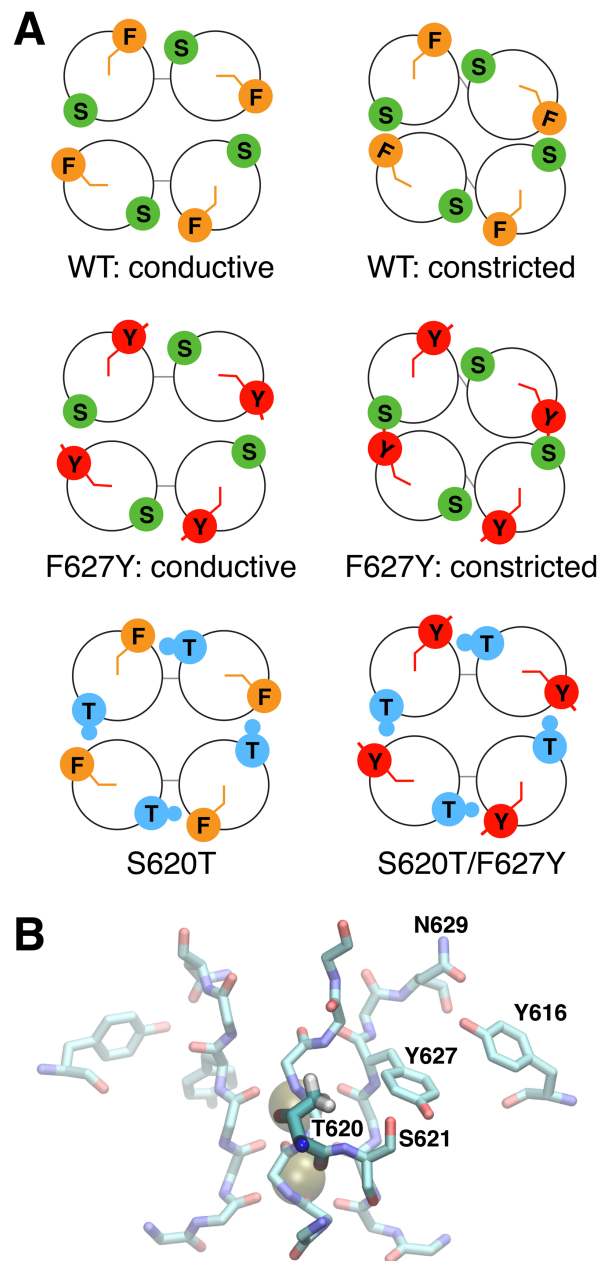


Fig. S6. The structural role of interaction between residues 620 and 627. **(A)** The schemes to show the inter-subunit contact between residues 620 and 627, and their structural role in the conductive-to-constricted transition for WT and mutants. The unfilled circles represent subunits of pore domain, and the solid dots respectively stands for S620 (green), T620 (blue), F627 (orange), and Y627 (red). The small blue dots represent the methyl groups of T620, and the sticks show either the backbone of residue 627 or the hydroxyl group of Y627 that could form hydrogen bond with S620. **(B)** The side view of a representative snapshot from the simulation of double mutant S620T/F627Y, to show the blockage of methyl group of T620 from the side-chain rotation of Y627.

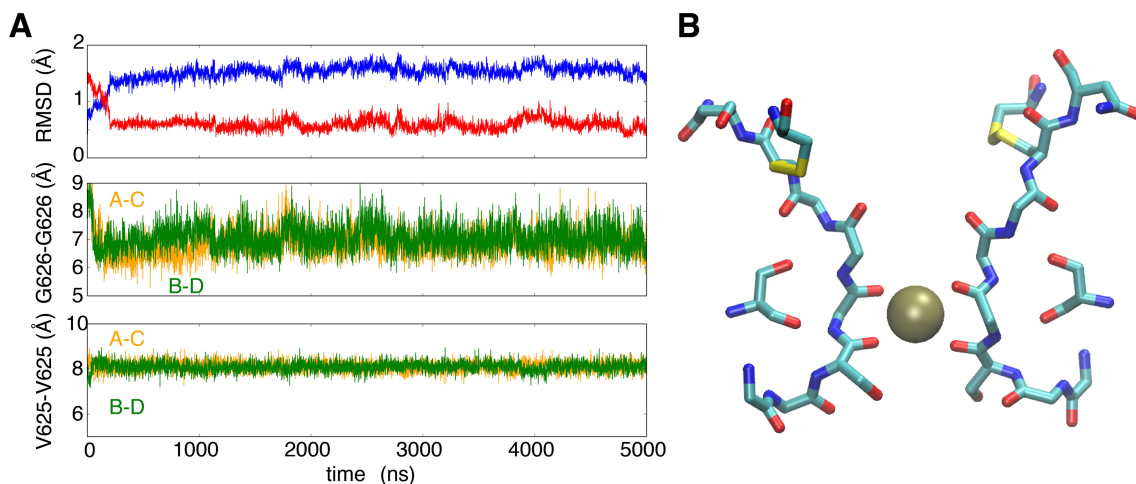


Fig. S7. MD simulation of double mutant G628C/S631C to lock the selectivity filter in an atypical conductive conformation with disulfide bond between residue C628 and C631 at the extracellular mouth of the filter. **(A)** Time series of the RMSDs (top panel) of the selectivity filter by using the initial (blue) or the last (red) structure as reference, and the cross-subunit distance between the Ca-Ca atoms of diagonally opposed subunits A and C (orange), and B and D (blue) for G626 (middle panel) and V625 (bottom panel). **(B)** The side view of the typical stable conformation of the double mutant G628C/S631C. For clarity, only two subunits are shown. See also Movies S1 and S2.

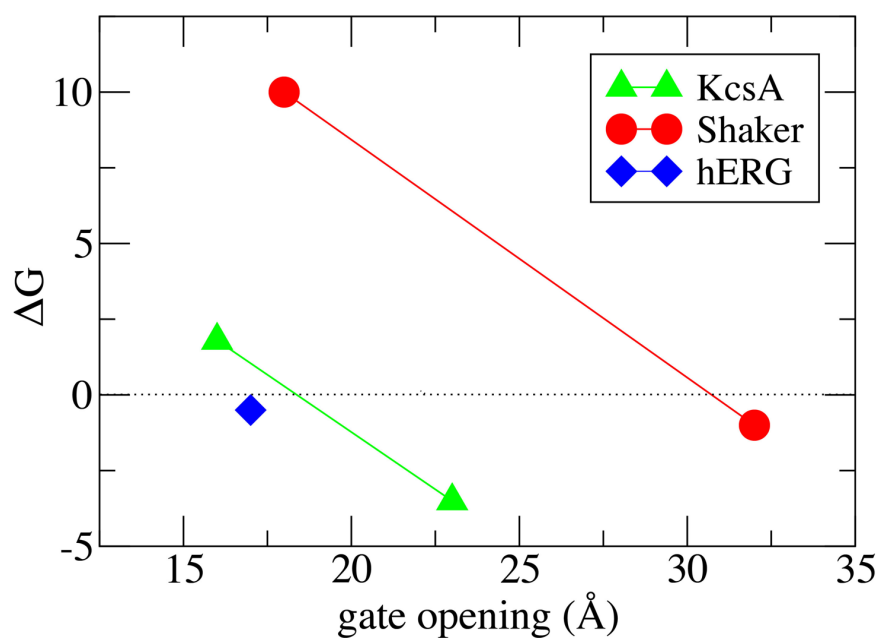


Fig. S8. Free energy difference between conductive and constricted states with different opening degrees of the intracellular gate. The free energy difference of KcsA is calculated based on two sets of PMFs respectively with gate opening as 16 and 23 Å in previous study (19). The data for *Shaker* channel is calculated based on two sets of PMFs respectively with gate opening as 18 and 32 Å. For hERG channel, there is only one PMF with gate opening as 17 Å.

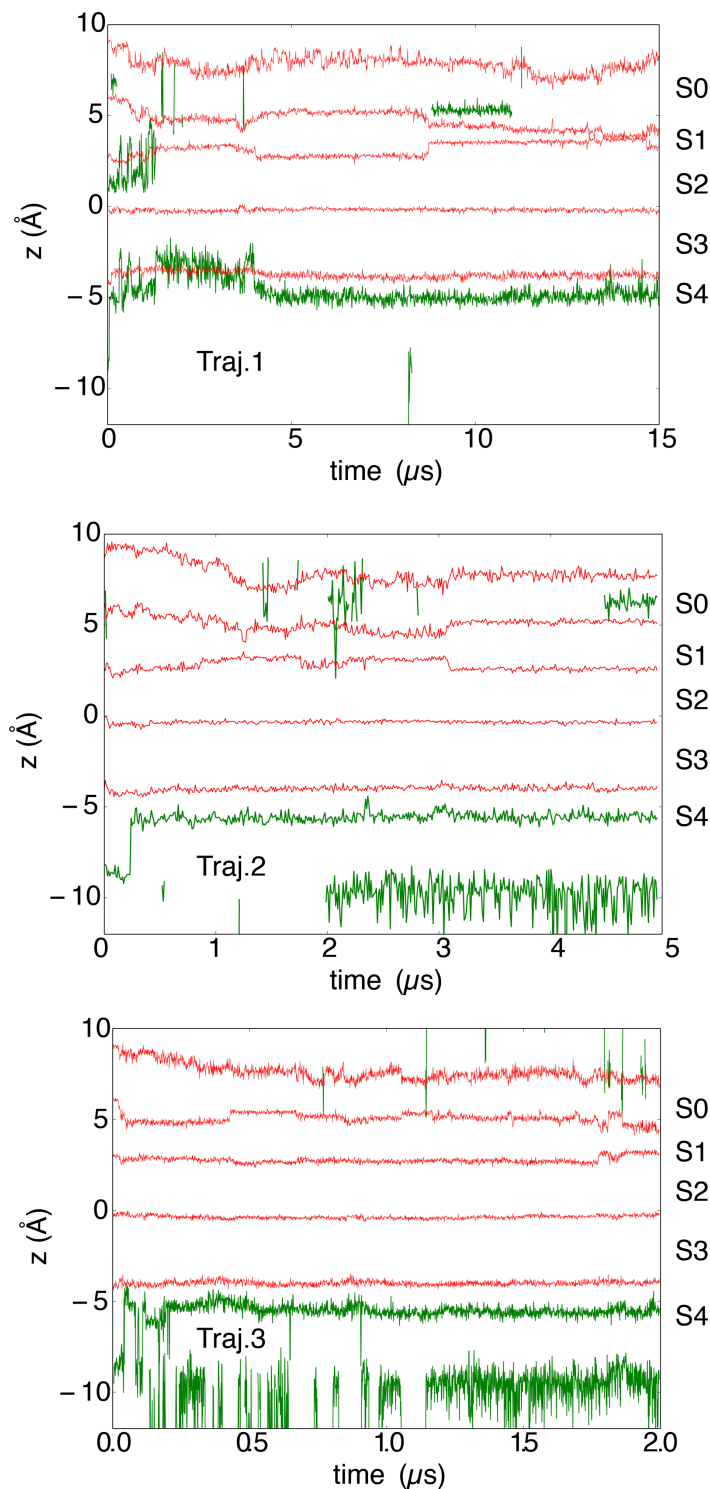


Fig. S9. The K⁺ ion occupancy in the simulations. The three unbiased simulations are the same as the Fig. S1. Traces of K⁺ ions (green) are shown through the selectivity filter, and the average z coordinates of carbonyl oxygens of G628, F627, G626, V625, and S624 are respectively shown in red lines to indicate the position of K⁺ binding sites (from S0 to S4 sites).

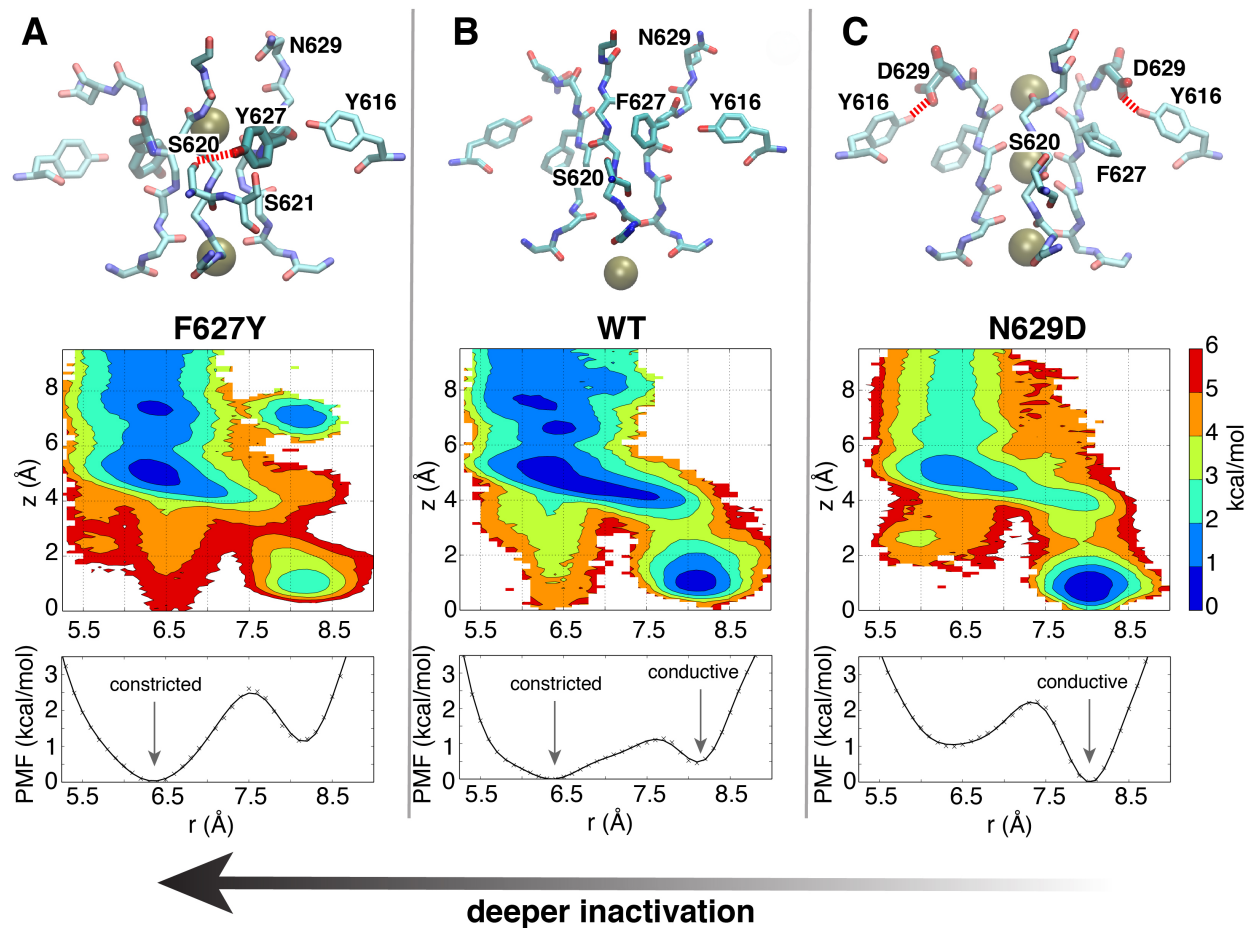


Fig. S10. 2D PMF to show the mutational effects of F627Y and N629D. The side view of representative conformation (top), 2D (middle) and 1D (bottom) PMFs for F627Y (A), wild type (B), and N629D (C). The comparison among the mutants and wild type shows an increasing of C-type inactivation from N629D, wild type, to F627Y. In 2D PMFs, the horizontal reaction coordinate r describes the width of the selectivity filter and is defined as the average cross-subunit pinching distance between the $C\alpha$ atoms of G626. The vertical reaction coordinate z indicates the position of the external K^+ ion along the z axis relative to the center of the selectivity filter. The 1D PMF is the one-dimensional PMF along horizontal reaction coordinate r , with integration of the vertical reaction coordinate z .

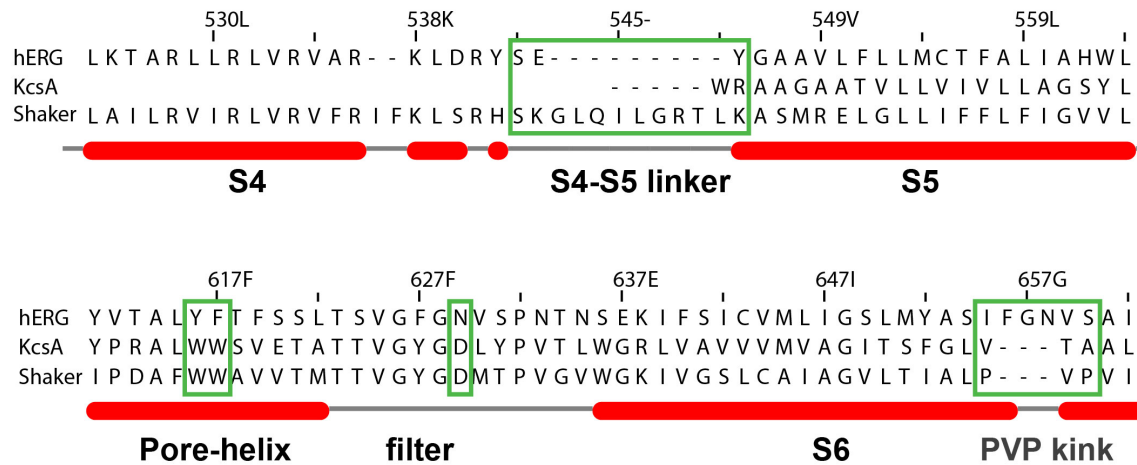


Fig. S11. Sequence alignment among hERG, KcsA and *Shaker* channels. The major sequence differences between hERG and *Shaker*, i.e., S4-S5 linker, PVP kink, “WW” motif, and N629, are highlighted, which are potentially relevant with the rapid C-type inactivation in hERG.